Photoconductivity experiments on superconducting Bi2Sr2CaCu2O8+x whiskers

Supercond. Sci. Technol. **20** (2007) 721–727 doi:10.1088/0953-2048/20/8/001

Photoconductivity experiments on superconducting $Bi_2Sr_2CaCu_2O_{8+x}$ whiskers

L Palumbo[1], S Cagliero[2], A Agostino[3], M Truccato[2], M G Medici[4] and P Volpe[3]

[1] NIS-Centre of Excellence, Dipartimento Chimica IFM Torino Università, Via P Giuria 7, I-10125 Torino, Italy
[2] NIS-Centre of Excellence, Dipartimento Fisica Sperimentale and CNISM UdR Torino Università, Via P Giuria 1, I-10125 Torino, Italy
[3] NIS-Centre of Excellence, Dipartimento Chimica Generale ed Organica Applicata and CNISM UdR Torino Università, Corso Massimo D'Azeglio 48, I-10125 Torino, Italy
[4] LPMC UMR 6622, Université de Nice Sophia Antipolis, Parc Valrose, F-06108 Nice, Cedex 02, France

E-mail: truccato@to.infn.it

Received 22 February 2007, in final form 30 April 2007
Published 12 June 2007
Online at stacks.iop.org/SUST/20/721

Abstract
In the present paper we report the results of photoconductivity experiments carried out in nearly optimally doped, single-phase $Bi_2Sr_2CaCu_2O_{8+x}$ (Bi-2212) whiskers. Samples with both straight and bent shapes have been investigated by means of the four-probe and two-probe configurations in dark and in illuminated conditions. Experimental data invariably show the absence of a persistent photoconductivity (PPC) effect. Such observations, combined with the very high crystal quality of the whiskers, which corresponds to the absence of defects acting as electron traps, can be explained in the framework of the electron–hole pair excitation model (Kudinov *et al* 1990 *Phys. Lett.* A **151** 358). In contrast, experimental data show a reversible increase of the electrical resistance under illumination, which is fully consistent with a local heating effect due to the thermal load induced by the light. Such resistance increase is especially large for samples measured in the two-probe configuration, suggesting a possible supplementary effect due to an interaction between the light and the *c*-axis resistivity or the contact resistance.

1. Introduction

Since the very first years after the discovery of high T_c superconductors (HTSC), it has been well known that irradiating oxygen-deficient $YBa_2Cu_3O_{6+x}$ (YBCO) thin films with visible light induces persistent photoconductivity (PPC) as well as persistent photoinduced superconductivity (PPS) [1, 2].

PPC is an interesting and unusual effect consisting of an electrical conductivity increase in some kinds of oxygen-deficient rare-earth cuprates (e.g. YBCO or $GdBa_2Cu_3O_y$) and manganites (e.g. $La_{2/3}Sr_{1/3}MnO_{3-\delta}$) due to illumination. This effect persists after the light is switched off until the material is heated above a characteristic temperature, which is sometimes as high as room temperature, and is more pronounced for highly underdoped samples [3].

Moreover, the interaction of visible light with oxygen-deficient rare-earth cuprates (RBaCuO) gives rise to a general improvement of their superconducting properties, producing for instance an increase of the critical temperature T_c and the critical current density j_c. Also this enhanced superconductivity relaxes towards the original properties of the materials only above some threshold temperature, typically less than 100 K, and is therefore named persistent photoinduced superconductivity (PPS). Both PPC and PPS are

more pronounced for UV or visible radiation and vanish in the IR range.

As far as the RBaCuO materials are concerned, measurements of the Hall effect have shown that the excited state corresponding to the persistent photoinduced phenomena is correlated with an increase of the carrier density [4]. Therefore, Kudinov *et al* [1] proposed a model suggesting that the sample illumination could result in a photoexcitation of electron–hole pairs across the YBCO bandgap. In this semiconductor-like picture, electrons are subsequently trapped by defects, which in poorly oxygenated samples correspond to the oxygen vacancies localized in the CuO chains, where otherwise, in fully oxygenated samples, an oxygen ion would be located. Such a capture process creates excess mobile holes transferred into extended states in the CuO_2 planes. The increase of carriers in these planes enhances the transport properties of the material. Clearly, this effect is more pronounced for oxygen-deficient films because the number of trapped electrons is proportional to the number of the oxygen vacant sites. Presently, this capture mechanism seems to be the model that probably best describes the PPC and PPS phenomena in materials where the CuO chains exist [4]. For review articles on the PPC and PPS effects on RBaCuO thin films, see, for example, Hoffmann *et al* [5] and Gilabert *et al* [4, 6].

As discussed above, according to Kudinov's model [1] the oxygen vacancies in the CuO chains play an essential role for the PPC. On the other hand, most of the HTSC are characterized by the absence of such chains, showing a multilayer structure with a regular stacking of CuO_2 planes connected by charge reservoir layers. Therefore, in principle, the importance of the CuO chains can be checked by performing PPC experiments in materials other than RBaCuO.

Similar experiments have been carried out in $Tl_2Ba_2CuO_{6+\varepsilon}$, where no CuO chain exists, by Hoffmann *et al* [7], showing the existence of PPC phenomena in this material. On the other hand, Gilabert *et al* [8] displayed effects of PPS in $Bi_2Sr_2CaCu_2O_{8+x}$ (Bi-2212) grain boundary tunnel junctions at low temperatures. Moreover, Baldovino [9] has measured a PPC effect at room temperature of the order of 2% in highly resistive Bi-2212 step edge junctions.

Such experimental results seem to suggest that the CuO chains are not an essential feature for PPC or PPS. Nevertheless, all of them have been obtained in polycrystalline systems, which are significantly influenced by the presence of highly defective regions like grain boundaries. In fact, Fujii *et al* [10–12] proved that such boundaries can show the presence of amorphous areas, whose features are controlled by the oxygen partial pressure during the crystallization process. On the other hand, the measurements by Prouteau *et al* [13] have shown that the grain boundaries are characterized by extended non-stoichiometric zones, depleted in oxygen, which has also been confirmed from an electronic point of view by the Josephson junction experiments on YBCO [6]. Therefore it is very likely that these defects could act as electron traps, just like the oxygen vacancies of the CuO chains in RBaCuO.

This means that Kudinov's model [1] can be more deeply tested by ruling out both kinds of electron trapping. To the best of our knowledge, no result of PPC experiments on single-crystal HTSC samples other than RBaCuO has been published until now. In the present paper we report our results for Bi-2212 whiskers, which are characterized by very high crystal quality and excellent superconducting properties [14].

2. Experimental details

The Bi-2212 whiskers were grown starting from high purity commercial powders of Bi_2O_3, $SrCO_3$, $CaCO_3$ and CuO (Aldrich 99.9999%) finely mixed in Bi:Sr:Ca:Cu stoichiometric ratios of 1.5:1:1:2. The mixture was melted at 1050 °C and glassy plates were produced by quenching the melt between copper plates at room temperature. Crystals grew from the plates during a five-day annealing at 855 °C in 100% O_2 gas flow.

Such conditions were selected in order to obtain whiskers with doping features corresponding to the nearly optimally doped or slightly overdoped state, in order to minimize the possible presence of defects due to oxygen vacant sites. X-ray diffraction (XRD) measurements performed on some of the resulting crystals showed that the c-axis lattice parameter was $c = 30.576 \pm 0.002$ Å. Such short values are usually associated with highly overdoped Bi-2212 structures [15–17], but in this case it should be considered that whiskers grown from glassy plates show a stoichiometric ratio Sr:Ca almost equal to 1 [18], which reduces the length of the c axis due to the smaller ionic radius of Ca compared to Sr [17, 19]. Therefore, it can be deduced that the whiskers grown for the present experiments were in the slightly overdoped state, which is also confirmed by a previous systematic study on the relationship between the c-axis lengths and the doping conditions in Bi-2212 whiskers [20].

The whiskers were selected under an optical microscope and mounted onto sapphire substrates. Only samples narrower than a few microns were selected at this stage, corresponding to cross-sectional areas of the order of 1 μm^2 or less, which are characterized by a very low density of defects like dislocations, growth steps and superstructure defects [21, 22]. Silver electrical contacts were evaporated through a steel mask in order to obtain the standard four-probe geometry. Further details on sample preparation can be found in [23].

The sample morphology and sizes were investigated by means of scanning electron microscopy (SEM) and atomic force microscopy (AFM). Typical crystal lengths are of the order of 700 μm, with 70 μm long voltage contacts spaced by about 100 μm, while the crystal width and thickness are of the order of 3 and 1 μm, respectively.

Preliminary electrical characterization of the crystals was performed in order to exclude the samples exhibiting evidence of intergrowths of the $Bi_2Sr_2Ca_2Cu_3O_{10+x}$ (Bi-2223) phase and therefore to select only single-phase whiskers of the pure Bi-2212 material. The corresponding resistance versus temperature behaviour $R(T)$ was measured in the 78–300 K range by means of an Oxford Instruments Optistat DN liquid nitrogen cryostat.

On the other hand, PPC experiments were performed by measuring both $R(T)$ and resistance versus time characteristics $R(t)$ in a Leybold RW5 closed circuit helium cryostat equipped with a quartz optical window. The samples were illuminated by means of a 70 W Hg–Xe lamp about 20 cm apart from the crystals, delivering a typical power density at the sample

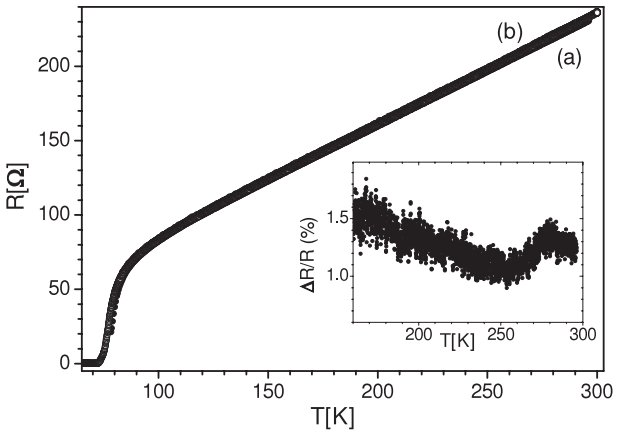

Figure 1. $R(T)$ characteristics of sample WLP15 measured immediately after the electrical contacting procedure (solid circles, curve (a)) and after nine-day ageing at −10 °C (open circles, curve (b)). The inset shows the relative increase of curve (b) with respect to curve (a) for the temperature region corresponding to the normal state resistance ($T > 160$ K).

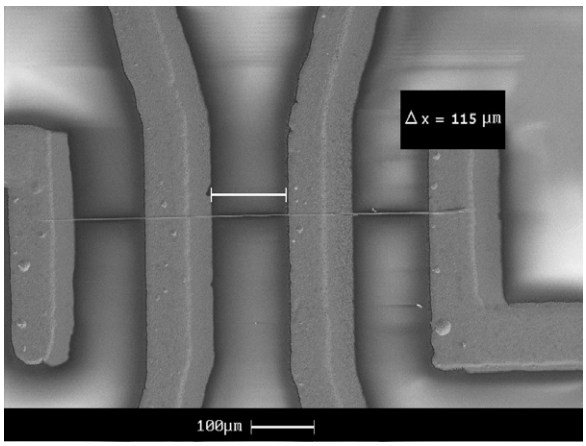

Figure 2. SEM micrograph of a typical sample with regular straight shape (WLP15). The whisker is the approximately horizontal line. A white bar indicates the voltage contact separation Δx and the corresponding measurement is reported in the box.

surface of the order of 1 W cm^{-2}. The lamp spectrum mainly consisted of a large ultraviolet and visible (UV–vis) component and only a minor infrared (IR) contribution. All photoconductivity measurements carried out on the Leybold system were performed only during heating ramps with the compressor powered off to avoid vibrations.

In order to minimize the effects due to the cation mobility and oxygen depletion already observed in Bi-2212 whiskers aged at room temperature [24], the samples were stored at about −10 °C between two subsequent measurements.

This procedure was quite effective in slowing down the crystal ageing process, as can be observed in figure 1, where the $R(T)$ curves corresponding to two different ageing times of the same crystal are displayed. Actually, even though curve (b) of figure 1 was measured after nine-days' storage since the measurement of curve (a), the two characteristics appear to be almost identical. By considering that the effect of thermodynamical fluctuations usually disappears in Bi-2212 whiskers for $T > 160$ K [25], the normal state resistance can be safely observed only in this temperature range. The inset of figure 1 shows that in this case the corresponding increase is of the order of 1%.

However, since the importance of the ageing process increases non-linearly in time [24, 26, 27], its possible effect on PPC measurements should be carefully considered in the data analysis.

3. Results and discussion

We performed photoconductivity experiments on two different sets of samples showing either typical or unusual features, from both the electrical and the morphological points of view.

3.1. Samples with linear geometry

Concerning the set with usual properties, which consisted of crystals with a very regular straight shape, a representative sample is displayed in figure 2, while its longitudinal and

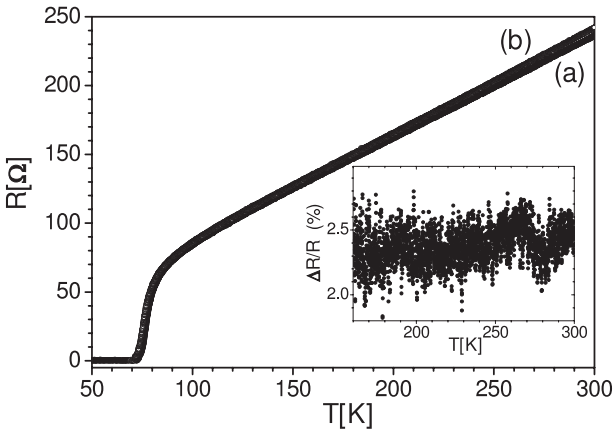

Figure 3. $R(T)$ characteristics of sample WLP15 measured in dark conditions (solid circles, curve (a)) and, in a subsequent experiment, under UV–vis irradiation (open circles, curve (b)). The inset displays the percentage increase of curve (b) with respect to curve (a) for the temperature region corresponding to the normal state ($T > 160$ K).

Table 1. Relevant sizes for a typical whisker sample (WLP15): voltage contact separation is indicated by Δx, voltage contact lengths by l_{V1} and l_{V2}, width and thickness by w and t, respectively.

Δx (μm)	l_{V1} (μm)	l_{V2} (μm)	w (μm)	t (nm)
115 ± 2	66 ± 2	61 ± 2	4.2 ± 0.3	541 ± 26

transverse sizes are reported in table 1. Moreover, its four-probe $R(T)$ measurements in dark and under illumination conditions are plotted in figure 3.

Both the values of the room-temperature resistivity ($\rho_{300} \approx 4.7 \times 10^{-6}$ Ω m) and the shape of the $R(T)$ curves reported in figure 3, which show no deviation from linearity down to 160 K, clarify that these as-grown crystals are nearly optimally doped [28]. Such a conclusion is also confirmed by the T_c values of this set of crystals, which are included in the range between 77.7 and 78.7 K, very close to the maximum T_c values for Bi-2212 whiskers reported in the systematic study of doping by Inomata *et al* [20]. Therefore this kind of sample

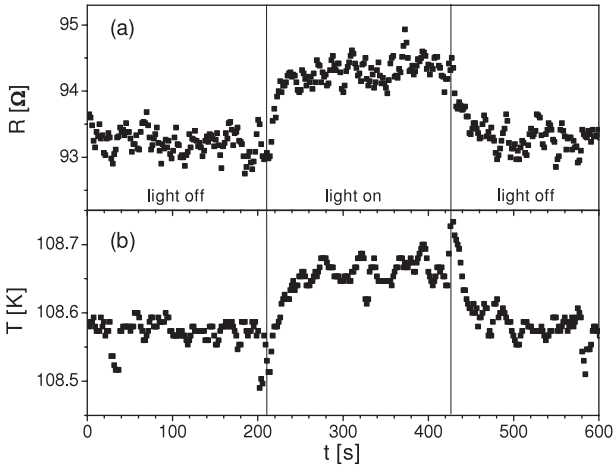

Figure 4. $R(t)$ characteristics for sample WLP15 (a) and temperature versus time monitoring $T(t)$ for the nearest thermometer (b), located a few millimetres apart. The nominal equilibrium temperature of the cold head was 110 K. Light switching on and off is indicated by vertical lines.

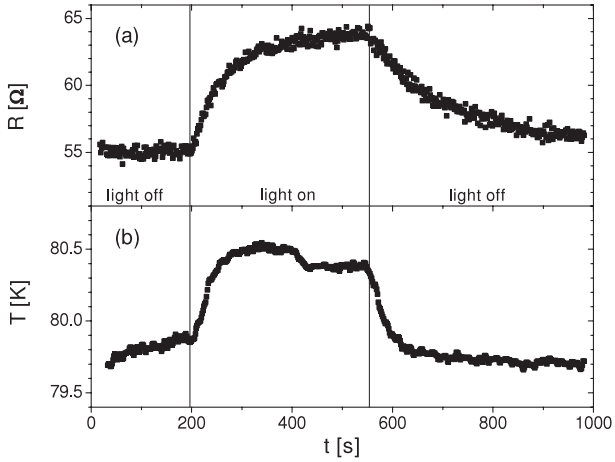

Figure 5. $R(t)$ characteristics for sample WLP15 (a) and $T(t)$ for the nearest thermometer (b), located a few millimetres apart. The nominal equilibrium temperature of the cold head was 80 K. Light switching on and off is indicated by vertical lines.

is a good candidate to test the presence of the PPC effect in systems with only a very low level of electron trapping.

Actually, it is apparent from the data of figure 3 that under illumination the whisker shows a resistivity increase, which is opposite to the PPC effect. In principle, this behaviour can be ascribed to two different reasons: (i) crystal ageing and (ii) possible sample heating due to irradiation.

Concerning the first phenomenon, the inset of figure 3 shows that curve (b) displays a percentage increase with respect to curve (a) that is temperature-independent in the range $T > 160$ K, which corresponds to the pure normal state behaviour. Since all the other microscopic quantities involved in the material resistivity $\rho = m^*/(ne^2\tau)$ are either constant (the effective mass m^* and the electronic charge e) or temperature-dependent (the relaxation time τ), this fact seems to suggest that a decrease occurred in the carrier concentration n of the material. Moreover, it is worth noting that a linear extrapolation based on the ageing rate already observed for the same sample in figure 1 gives an expected resistance increase of about 0.7%. The fact that the average resistance increase observed in figure 3 is remarkably greater (≈2.4%) gives further evidence in favour of the ageing process, which is related to kinematic factors and non-linear in time [27].

We therefore conclude that the resistance increase observed in the $T > 160$ K region of figure 3 is due to the crystal ageing. However, such a conclusion cannot be drawn by the resistance behaviour at lower temperatures because thermodynamical fluctuations deeply modify the electrical properties of the material in a non-trivial way [25].

Regarding possible sample heating due to the thermal load provided by the light source during illumination, this phenomenon was directly investigated by placing a thermometer as near as possible (≈8 mm) to the sample position and by monitoring its temperature along with the sample resistance while switching on and off the light source.

Figures 4 and 5 display the results of such measurements for the nominal equilibrium temperatures of 110 and 80 K, respectively. These data were acquired immediately before the $R(T)$ acquisition of curve (a) in figure 3, during exactly the same thermal cycle, in order to minimize the ageing effect on the crystal between the two kinds of measurements.

It is apparent that, in both cases, both a resistance and a temperature increase can be observed when switching the light source on and that this effect disappears when switching it off.

In more detail, it is possible to observe that in the closest neighbourhood of the sample the temperature increases by 0.1 and 0.7 K at the nominal temperatures of 110 and 80 K, respectively (figures 4(b) and 5(b)). On the other hand, the thermometer used for monitoring the cold head of the system, which was located in a copper block about 22 mm apart from the sample, was not able to detect any temperature variation, at least down to our sensitivity level of 0.02 K. It is also clear that the resistance increase by 1.1 and 8.6 Ω of figures 4(a) and 5(a), respectively, occurs simultaneously with the above-mentioned heating of the sample neighbourhood. Such a resistance increase can be translated into a temperature one by comparing it to the proper region of the $R(T)$ characteristic of figure 3(a). Sample temperature increases $\Delta T_s = 1.3$ and 3.2 K at the nominal temperatures of 110 and 80 K, respectively, can be determined in this way. This clarifies that a non-homogeneous temperature field is induced in the copper sample holder by the light source. Its characteristic decrease length l can be estimated in both cases by assuming an exponential decay law for the temperature as a function of the distance from the light spot position, and this results in $l_{110} = 3.0$ mm and $l_{80} = 5.4$ mm for the nominal temperatures of 110 and 80 K, respectively. It is worth mentioning that both of these lengths are compatible with the fact that no temperature increase is observable at the distance of 22 mm from the sample. These results lead to the conclusion that both ΔT_s and l increase when decreasing the average temperature of the system, indicating that stronger non-equilibrium conditions are reached when illuminating the sample at lower temperatures. This observation also agrees with the remarkable decrease of the copper specific heat in this temperature range. On the other hand, when increasing the average temperature of the system above ≈140 K, the specific heat increase of copper should

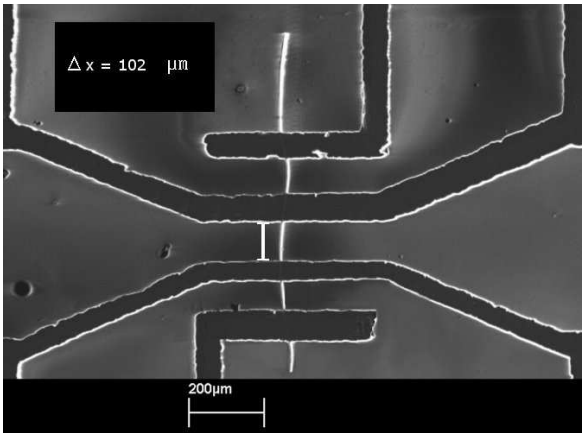

Figure 6. SEM micrograph of a typical sample with irregularly bent shape (WLP3). The whisker is the approximately vertical white line. A white bar indicates the voltage contact separation Δx and the corresponding measurement is reported in the box.

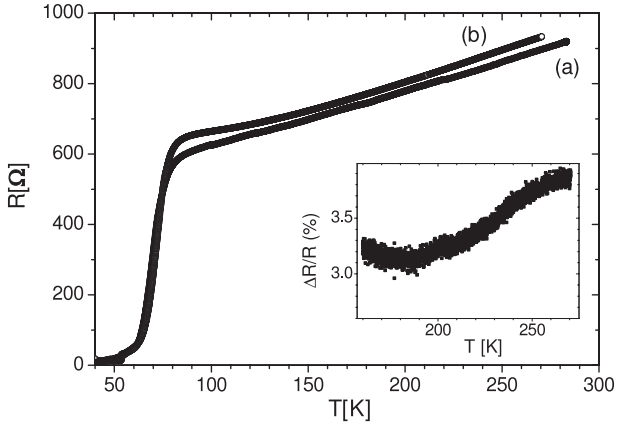

Figure 7. $R(T)$ characteristics of sample WLP3 measured in dark conditions (solid circles, curve (a)) and, in a subsequent experiment, under UV–vis irradiation (open circles, curve (b)). The inset displays the percentage increase of curve (b) with respect to curve (a) for the temperature region corresponding to the normal state ($T > 160$ K).

induce a vanishing effect on the sample holder. Actually, neither temperature nor resistance variation could be observed in this temperature region.

Therefore, we conclude that both the crystal ageing and the sample heating due to irradiation determine the resistance increase observed in curve (b) in figure 3, the former dominating in the high-temperature and the latter in the low-temperature region. The PPC effect, if present, certainly has a very small intensity, which is easily obscured by the two previous phenomena.

3.2. Samples with non-linear geometry

Figure 6 shows the typical shape of the set of samples with a non-linear geometry, as resulting from SEM observation. Further detailed investigation carried out by AFM has revealed that the crystal cross section can be described as two neighbouring rectangles sharing the same baseline.

The lengths of the crystal portions relevant to the electrical measurements are reported in table 2, along with the sizes of the two rectangles forming the cross section. It is worth mentioning that the crystal originally grew along a straight line and that the bent shape arose during the electrical contacting procedure because of the interaction between the metal mask and the crystal itself.

By evaluating the minimum curvature radius of the sample in about 180 μm, it is possible to estimate the maximum crystal strain as about 0.36%. It has been shown by Matsubara *et al* [29] that in Bi-2212 whiskers no variation can be detected in T_c for strains up to 0.5%, even if the J_c values start decreasing for strains above 0.3–0.4%. Therefore, even if the morphological features of these whiskers are not typical, no significant difference can be expected in their electrical properties with so small strain values.

Since we were not able to obtain samples with larger strains, we decided to test them in a two-probe configuration. This clearly introduces in the measurements also the contact resistance of the two probes as two additional ohmic resistances in series with the crystal resistance. Such resistance has been measured in almost identical samples by Aukkaravittayapun *et al* [30] by means of a three-terminal technique, showing that fresh Ag contacts have a typical resistance of 1–2 Ω in single Bi-2212 phase crystals and that it increases by about one order of magnitude with thermally cycling between room and liquid nitrogen temperatures several times. Such resistance values have been confirmed by our measurements in the temperature region below T_c, where the residual resistance due to each contact can be estimated in 4–7 Ω, depending on the thermal cycle. According to the average resistance values of our samples, this corresponds to a spurious contribution to the total resistance of the order of 1–2%.

It should be noted that, in principle, the electrical resistance of the two Ag metal strips providing electrical contacts to the crystals also contributes to the total resistance measurement in the two-probe configuration. However, the strip resistance was measured during a properly designed experiment, finding that it changes from 0.05 to 0.11 Ω in the temperature range corresponding to our experiment. This corresponds to a maximum percentage contribution less than 0.02% and can be safely neglected.

Therefore, the most interesting feature of the two-probe measurement is the fact that a contribution from the *c*-axis resistivity component arises in the voltage drop, as a consequence of the fact that the current is injected in the crystals along the *c*-axis direction in the same region where the voltage is measured. This problem has been accurately analysed by Esposito *et al* [31], who have shown that both the *ab*-plane resistivity component ρ_{ab} and its *c*-axis counterpart ρ_c are involved in any voltage measurement and that their disentanglement can be obtained only in a four-probe configuration when the condition $L \gg \pi t\sqrt{\rho_c/\rho_{ab}}$ is satisfied, where L is the total crystal length and t is its thickness.

Figure 7 reports the $R(T)$ measurements of a representative sample of this series both in dark conditions and under UV–vis irradiation. The most important feature is the appearance in the data of an upwards curvature, which is present both in dark and in illuminated conditions, even if it is much more pronounced in the latter. This behaviour clearly resembles the typical one of ρ_c as a function of temperature [32] and

Table 2. Relevant sizes for an unusually bent whisker sample (WLP3): voltage contact separation is indicated by Δx, voltage contact lengths by l_{V1} and l_{V2}. Width and thickness of the first rectangle forming the cross section are indicated by w_1 and t_1, respectively, while w_2 and t_2 are the width and thickness of the second rectangle.

Δx (μm)	l_{V1} (μm)	l_{V2} (μm)	w_1 (μm)	w_2 (μm)	t_1 (nm)	t_2 (nm)
102 ± 3	75 ± 2	57 ± 2	0.95 ± 0.07	0.34 ± 0.04	676 ± 17	319 ± 30

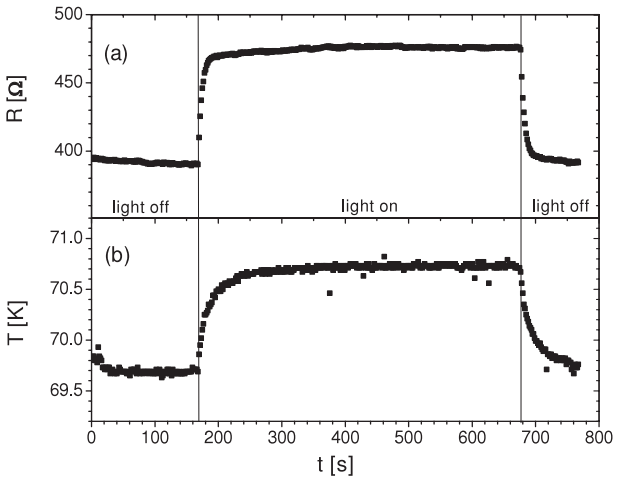

Figure 8. $R(t)$ characteristics for sample WLP3 (a) and $T(t)$ for the nearest thermometer (b), located a few millimetres apart. The nominal equilibrium temperature of the cold head was 70 K. Light switching on and off is indicated by vertical lines.

is exactly the same as other measurements that have been interpreted in the past as pure ρ_{ab} determinations [33]. This fact testifies that a ρ_c contribution can be easily introduced in the resistivity measurements when departing from ideal geometry. The fact that ρ_c significantly contributes to the resistance measurement is further confirmed by the very high room-temperature resistivity ($\rho_{300} \approx 7 \times 10^{-6}$ Ω m) which is not accompanied by an extended pseudogap region, contrary to what one should expect from Watanabe *et al* [28].

The data of figure 7(b) demonstrate that also for this series of samples the behaviour under illumination is contrary to the PPC effect. In fact, the total effective resistivity increases and the ρ_c contribution is enhanced in importance, as can be deduced by the increased curvature. Moreover, the inset highlights that the effective resistivity increase is clearly temperature-dependent.

Among the temperature-dependent phenomena, heating by the lamp certainly affects these measurements. This is proved by the $R(t)$ characteristics shown in figure 8, where a simultaneous increase of the sample resistance and of the nearest thermometer can be observed. However, it has already been mentioned above that in our system such an effect becomes negligible at temperatures as high as 140 K or above, which rules out any influence on the temperature range corresponding to the inset of figure 7. Even below this temperature, it is very unlikely that heating can be the origin of the resistance increase under illumination, because of its large extent of about 7% at $T \approx 90$ K.

On the other hand, it has already been clarified in the past that oxygen depletion is induced at the Ag/Bi-2212 interface by the presence of the metal contacts [34] and that such a phenomenon adds to or promotes the natural instability of the BSCCO whiskers [24, 26]. However, only a temperature-independent increase of the *ab*-plane resistance can be expected from the reduction in the carrier density resulting from such processes.

Since in our two-probe measurements both the contacts and the ρ_c contribute to the total effective resistance, the results of figure 7 suggest that either of them could be affected by light in a temperature- dependent way. Further investigation is needed to determine the contribution of each of them to such resistance increase.

4. Conclusions

We investigated the in-plane photoconductivity on two different series of nearly optimally doped samples showing either typical straight or unusually bent shapes. We have detected no PPC effect on both kind of samples. Such results are compatible with the hypothesis by Kudinov *et al* [1] that the absence of sources for electron trapping inhibits the appearance of PPC. In contrast, we observed a small resistance increase induced by heating due to light irradiation.

Moreover, for the samples measured in a two-probe configuration we found a resistance increase whose origin is still not clear. Further investigation is necessary to assess the role of the out-of-plane resistivity and of the electrical contacts in such an effect.

References

[1] Kudinov V I, Kirilyuk A I, Kreines N M, Laiho R and Lähderanta E 1990 *Phys. Lett.* A **151** 358
[2] Nieva G, Osquiguil E, Guimpel J, Maenhoudt M, Wuyts B, Bruynseraede Y, Maple M B and Schuller I K 1992 *Appl. Phys. Lett.* **60** 2159
[3] Gilabert A, Cauro R, Contour J P, Medici M G, Grenet J C, Papiernik R and Schuller I K 2000 Superconducting and related oxides: physics and nanoengineering *Proc. SPIE* **4058** 331
[4] Gilabert A, Hoffmann A, Medici M G and Schuller I K 2000 *J. Supercond.* **13** 1
[5] Hoffmann A, Reznik D and Schuller I K 1997 *Adv. Mater.* **9** 271
[6] Gilabert A, Hoffmann A, Elly J, Medici M G, Seidel P, Schmidl F and Schuller I K 1997 *J. Low Temp. Phys.* **106** 255
[7] Hoffmann A, Schuller I K, Ren Z, Lao J Y and Wang J H 1997 *Phys. Rev.* B **56** 13742
[8] Gilabert A, Plecenik A, Medici M G, Grajcar M, Karlovsky K and Dittman R 1999 *Appl. Phys. Lett.* **74** 3869
[9] Baldovino S 1999 Effetti dell'illuminazione sulle proprietà di trasporto dei film di BSCCO ($Bi_2Sr_2Ca_nCu_{2n}O_{4n+2}$) *Master Thesis* Torino University unpublished
[10] Fujii H, Kitaguchi H, Kumakura H and Togano K 1997 *Physica* C **282** 2567

[11] Fujii H, Kumakura H, Kitaguchi H, Togano K, Zhang W, Feng Y and Hellstrom E E 1997 *IEEE Trans. Appl. Supercond.* **7** 1707
[12] Fujii H, Kumakura H and Togano K 1999 *J. Mater. Res.* **14** 349
[13] Prouteau C, Duscher G, Browning N D and Pennycook S J 1998 *Physica* C **298** 1
[14] Latyshev Y, Gorlova I, Nikitina A, Antokhina V, Zybtsev S, Kukhta N and Timofeev V 1993 *Physica* C **216** 471
[15] Xenikos D G and Strobel P 1995 *Physica* C **248** 343
[16] Kendziora C, Kelley R J, Skeltom E and Onellion M 1996 *Physica* C **257** 74
[17] Emmen J H P M, Lenczowski S K J, Daalderop J H J and Brabers V A M 1992 *J. Cryst. Growth* **118** 477
[18] Matsubara I, Funahashi R, Ueno K and Ishikawa H 2000 *Mater. Res. Bull.* **35** 441
[19] Han S H, Gu G D, Shao Y, Russell G J and Koshizuka N 1995 *Physica* C **246** 22
[20] Inomata K, Sato S, Nakajima K, Kim S J, Hatano T, Takano Y, Nagao M and Yamashita T 2004 *Physica* C **412–414** 1396
[21] Timofeev V N and Gorlova I G 1998 *Physica* C **309** 113
[22] Gorlova I G and Timofeev V N 1995 *Physica* C **255** 131
[23] Truccato M, Rinaudo G, Manfredotti C, Agostino A, Benzi P, Volpe P, Paolini C and Olivero P 2002 *Supercond. Sci. Technol.* **15** 1304
[24] Truccato M, Lamberti C, Prestipino C and Agostino A 2005 *Appl. Phys. Lett.* **86** 213116
[25] Truccato M, Agostino A, Rinaudo G, Cagliero S and Panetta M 2006 *J. Phys.: Condens. Matter* **18** 8295
[26] Truccato M, Cagliero S, Agostino A, Panetta M and Rinaudo G 2006 *Supercond. Sci. Technol.* **19** 1003
[27] Cagliero S, Agostino A, Bonometti E and Truccato M 2007 *Supercond. Sci. Technol.* **20** 667
[28] Watanabe T, Fujii T and Matsuda A 1997 *Phys. Rev. Lett.* **79** 2113
[29] Matsubara I, Kageyama H, Tanigawa H, Ogura T, Yamashita H and Kawai T 1989 *Japan. J. Appl. Phys.* **28** L1121
[30] Aukkaravittayapun S, Benedict K, Gorlova I, King P, Latyshev Y, Staddon C and Zybtsev S 1995 *Supercond. Sci. Technol.* **8** 718
[31] Esposito M, Muzzi L, Sarti S, Fastampa R and Silva E 2000 *J. Appl. Phys.* **88** 2724
[32] Wahl A, Thopart D, Villard G, Maignan A, Simon Ch, Soret J C, Ammor L and Ruyter A 1999 *Phys. Rev.* B **60** 12495
[33] Badèche T, Monnereau O, Ghorayeb A, Grachev V and Boulesteix C 1995 *Physica* C **241** 10
[34] Luo Y S, Yang Y N and Weaver J H 1992 *Phys. Rev.* B **46** 1114